

A Computational Study of the Decomposition of Carbon Tetrafluoride in Wet Argon under Electron Beam Irradiation

Susumu KATO, Isao OKUDA, Eiichi TAKAHASHI and Yuji MATSUMOTO

National Institute of Advanced Industrial Science and Technology (AIST), Tsukuba, Ibaraki 305-8568, Japan

(Received 14 March 2008 / Accepted 4 June 2008)

In this study, a computational method of the kinetic model of carbon tetrafluoride (CF₄) in wet argon gas under electron beam irradiation was developed. Using this method, the mechanism of decomposition and the optimum concentration of H₂O during decomposition of CF₄ was determined. It was found that 99% of 1000 ppm of CF₄ of in atmospheric-pressure argon gas decomposed at an input energy density of 1 J/cm³.

© 2008 The Japan Society of Plasma Science and Nuclear Fusion Research

Keywords: decomposition of per-fluorocompounds, electron beam irradiation, nonthermal plasma, kinetic model

DOI: 10.1585/pfr.3.038

1. Introduction

The removal of per-fluorocompounds (PFCs), such as CF₄ and C₂F₆, is important for the abatement of greenhouse gases from a semiconductor facility. Non-thermal plasma technology has been applied to the decomposition of PFCs [1]. In non-thermal plasmas, electron impact reactions and ion reactions with PFCs are the dominant decomposition processes, because PFCs are inherently inert to radicals.

A non-thermal plasma is usually generated by a discharge. In non-thermal discharge plasmas, it is thought that electron impact dissociative reactions dominate the PFC decomposition processes [1]. High-current electron beams (e-beams) may possibly be employed to generate a non-thermal plasma. E-beams are frequently used in excimer lasers and radiation chemical reactions. An e-beam generated plasma has also been used for the decomposition of carbon tetrachloride [2]. Ions and metastable atoms are efficiently generated using an e-beam. The ion reaction for any PFC will be the dominant decomposition process [3,4], because the energy of secondary electrons produced by the e-beam rapidly decreases to room temperature.

The aim of this study was to determine the decomposition path for PFCs through e-beam generated plasma technology, and to evaluate its theoretical efficiency. We developed a kinetic model of the decomposition of CF₄ in wet argon under e-beam irradiation and determined the optimum concentration of H₂O required for the decomposition process. H₂O is employed as an additive for PFC abatement. Nitrogen and argon are important gases for most applications. The reaction of argon is fairly well understood, compared to the reaction of nitrogen.

2. Decomposition Mechanisms of CF₄

In non-thermal discharge plasmas, electron impact dissociative reactions, namely dissociative ionization, dissociation, and electron attachment, are the dominant decomposition processes of CF₄. The reactions are listed in Table 1.

Ions and metastable atoms are more efficiently generated in e-beam generated plasmas compared to discharge plasmas. The secondary electron temperature rapidly decreases to room temperature. Therefore, the dominant decomposition processes of CF₄ are reactions with the ions and metastable atoms of argon; these reactions are listed in Table 2. The reactions of radicals with PFC molecules are less important, because of their relatively small reaction rate coefficients.

The electron attachment reaction of CF₄, with a cross-section peak of about 7 eV, will occur because secondary electrons have an average energy of about 7 eV for argon [6]. Attachments will be minor events in e-beam generated

Table 1 Electron impact dissociative reaction processes, where the threshold electron energy is lower than 30 eV.

Reaction	E_{th} (eV)	Ref.
Dissociative ionization		
$CF_4 + e^- \rightarrow CF_3^+ + F + 2e^-$	16	[5]
$CF_4 + e^- \rightarrow CF_2^+ + 2F + 2e^-$	21	[5]
$CF_4 + e^- \rightarrow CF^+ + 3F + 2e^-$	26	[5]
Dissociation		
$CF_4 + e^- \rightarrow CF_3 + F + e^-$	13	[5]
$CF_4 + e^- \rightarrow CF_2 + 2F + e^-$	17	[5]
$CF_4 + e^- \rightarrow CF + 3F + e^-$	18	[5]
Electron attachment		
$CF_4 + e^- \rightarrow CF_3 + F^-$	4.65	[5]
$CF_4 + e^- \rightarrow CF_3^- + F$	5.4	[5]

author's e-mail: s.kato@aist.go.jp

Table 2 Ion and radical reaction processes.

Reaction	Rate (cm ³ s ⁻¹)	Ref.
Ion charge exchange		
CF ₄ + Ar ⁺ → CF ₃ ⁺ + F + Ar	7.0×10 ⁻¹⁰	[7]
CF ₄ + O ⁺ → CF ₃ ⁺ + OF	1.4×10 ⁻⁹	[8, 9]
CF ₄ + CO ⁺ → products	7.6 × 10 ⁻¹⁰	[10]
CF ₄ + O ₂ ⁺ → small reaction	< 3 × 10 ⁻¹²	[11]
CF ₄ + CO ₂ ⁺ → small reaction	~ 0	[10]
CF ₄ + H ₂ O ⁺ → small reaction	< 5 × 10 ⁻¹²	[12]
Radical Dissociation		
CF ₄ + Ar* → products	4 × 10 ⁻¹¹	[13, 14]
CF ₄ + O(¹ D) → CF ₄ + O(³ P)	≤ 1.3 × 10 ⁻¹³	[15]

plasmas because the energy of secondary electrons rapidly decreases to room temperature. Furthermore, electron impact ionization and dissociation by secondary electrons are also minor events.

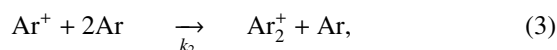
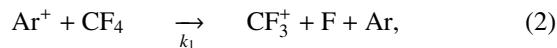
The G-values (molecules/100 eV) of argon are as follows [6]:

$$4.89\text{Ar} \xrightarrow{100\text{eV}} 1.08\text{Ar}^* + 3.82\text{Ar}^+ + 3.82\text{e}^-, \quad (1)$$

where Ar⁺ and Ar* are the argon ion and metastable Ar(³P_{0,2}). Ar⁺ and Ar* have an energy of about 16 and 12 eV, respectively. Both Ar⁺ and Ar* are capable of decomposing CF₄ as shown in Table 2. Hereafter, Ar⁺ and Ar* are called the activated species of argon. Input energy of 70% or more is used to produce the activated species of argon.

An e-beam with input energy density of 1 J/cm³ generates Ar⁺ ≈ 2.39 × 10¹⁷ cm⁻³ and Ar* ≈ 6.75 × 10¹⁶ cm⁻³. The density of the activated species of argon corresponds to 1.25% of the atmospheric-pressure gas density. Therefore, 1.25% of CF₄ in atmospheric-pressure argon gas is decomposed if all of the activated species of argon contribute to the decomposition process. However, many activated species of argon are quenched due to recombination, de-excitation, and radiation, and by the additives H₂O, O₂, H₂, intermediates, and by-products.

The decomposition of CF₄ and the major processes are,



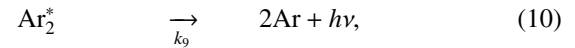
where $k_1 = 7.0 \times 10^{-10} \text{ cm}^3/\text{s}$ [7], $k_2 = 0.7 \times 10^{-31} \text{ cm}^6/\text{s}$ [16], and k_3 is dependent on the species M, and k_3 is typically 0 to less than 10⁻⁹ cm³/s. M represents the additives H₂O, O₂, and H₂, and the by-products.



where $k_4 = 9.1 \times 10^{-7} \times (T/300 \text{ K})^{-0.61} \text{ cm}^3/\text{s}$ [17] and k_5 is dependent on the species M (k_5 is typically 0 to less than 10⁻⁹ cm³/s).



where $k_6 = 4.0 \times 10^{-11} \text{ cm}^3/\text{s}$ [14], $k_7 = 1.0 \times 10^{-32} \text{ cm}^6/\text{s}$ [18], and k_8 is dependent on the species M (k_8 is typically 0 to less than 10⁻¹⁰ cm³/s).



where $k_9 = 6.0 \times 10^6 \text{ s}^{-1}$ [19] and k_{10} is dependent on the species M (k_{10} is typically 0 to less than 10⁻¹⁰ cm³/s).

The corresponding rate equations of the CF₄ decomposition are

$$\frac{d[\text{CF}_4]}{dt} = -\{k_1[\text{Ar}^+] + k_6[\text{Ar}^*]\}[\text{CF}_4] - \sum R_d[\text{CF}_4], \quad (12)$$

$$\frac{d[\text{Ar}^+]}{dt} = -k_1[\text{CF}_4][\text{Ar}^+] - \{k_2[\text{Ar}]^2 + \sum k_3[\text{M}]\}[\text{Ar}^+], \quad (13)$$

$$\frac{d[\text{Ar}^*]}{dt} = -k_6[\text{CF}_4][\text{Ar}^*] - \{k_7[\text{Ar}]^2 + \sum k_8[\text{M}]\}[\text{Ar}^*]. \quad (14)$$

The second term on the right hand side of Eq. (12) corresponds to another decomposition reaction, such as electron impact, which is not effective in e-beam generated plasmas. Therefore, the contribution of this reaction type is not included in our kinetic model. The decomposition rates of CF₄ by Ar⁺ and Ar* are defined by

$$DR_{\text{Ar}^+} = \frac{k_1[\text{CF}_4]}{k_1[\text{CF}_4] + k_2[\text{Ar}]^2 + \sum k_3[\text{M}]}, \quad (15)$$

and

$$DR_{\text{Ar}^*} = \frac{k_6[\text{CF}_4]}{k_6[\text{CF}_4] + k_7[\text{Ar}]^2 + \sum k_8[\text{M}]}. \quad (16)$$

The reaction diagram for CF₄ at a concentration of 1000 ppm (0.1%) in an e-beam irradiated argon gas at the standard temperature and pressure, and an input energy density of 20 mJ/cm³, is shown in Fig. 1. Here, $DR_{\text{Ar}^+} = 0.27$ and $DR_{\text{Ar}^*} = 0.13$ were obtained as additives, and the amounts of any by-products were small compared to the CF₄ concentration. As a result, about 25% of the input energy was used in the decomposition of CF₄ and about 2 × 10¹⁵ cm⁻³ of CF₄ molecules were decomposed. This value is the ideal limit, and decreases through the reaction of the activated species with additives and by-products.

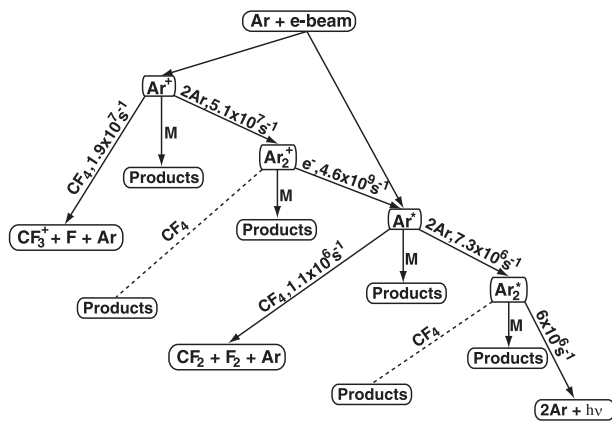


Fig. 1 Reaction diagram for CF_4 in e-beam irradiated argon gas at standard temperature and pressure (273.15 K and 10^5 Pa). The number density of CF_4 is $2.7 \times 10^{16} \text{ cm}^{-3}$. The input energy density is 20 mJ/cm^3 . The number density of Ar^+ and electron is $5 \times 10^{15} \text{ cm}^{-3}$. The reaction particle and reduction rates are shown on the arrows. Smaller contributions are presented as dotted lines. M represents the H_2O additives and by-products.

The energies of bimolecular-ion Ar_2^+ and dimer Ar_2^* of argon are 14.5 and 11 eV, respectively. The energies are greater than the ionization and dissociation energies of CF_4 . However, the decomposition of CF_4 by Ar_2^+ and Ar_2^* has not been confirmed experimentally. The decomposition of CF_4 by Ar_2^+ may be negligible even if Ar_2^+ can operate in the decomposition of CF_4 , because Ar_2^+ rapidly dissociates to Ar^* and Ar through dissociative recombination. The decomposition of CF_4 by Ar_2^* may be also negligible even if Ar_2^* can operate in the decomposition of CF_4 , because Ar_2^* rapidly dissociates to Ar^* and Ar through radiation emission.

3. The Simulation Model

The implemented numerical method employs a zero-dimensional kinetic model of the gas phase, because the e-beam can generate a uniform plasma. Input energy density per pulse in pulse operation is typically 20 mJ/cm^3 [20]. The temperature rise is about 50 degrees without radiation loss. In the model, reaction rates at room temperature are used for simplicity.

The reaction of Ar^+ , Ar^* , Ar_2^+ , and Ar_2^* with CF_4 and H_2O and other reactions related to by-products, are included in the model. The quenching reaction of the activated species with the minor intermediate and final products is not included. The reaction of Ar_2^+ and Ar_2^* with CF_4 is not included in the simulation. The reasons are discussed in the previous section. Typical reactions are listed in Tables 3, 4, 5, 6, and 7. Compositions of hydrocarbon and fluorinated hydrocarbon similar to $\text{C}_x\text{H}_y\text{F}_z$ ($x > 1, y > 1, z > 0$) are neglected because the composition rate is very small compared to the other reaction rates

Table 3 Ion-molecule reaction processes.

Reaction	Rate (cm^3/s)	Ref.
$\text{CF}_4 + \text{Ar}^+ \rightarrow \text{CF}_3^+ + \text{F} + \text{Ar}$	7.0×10^{-10}	[7]
$\text{CF}_3 + \text{Ar}^+ \rightarrow \text{CF}_3^+ + \text{Ar}$	1.0×10^{-10}	estimated
$\text{CF}_3 + \text{Ar}^+ \rightarrow \text{CF}_2^+ + \text{F} + \text{Ar}$	1.0×10^{-10}	estimated
$\text{CF}_2 + \text{Ar}^+ \rightarrow \text{CF}_2^+ + \text{Ar}$	1.0×10^{-10}	estimated
$\text{CF}_2 + \text{Ar}^+ \rightarrow \text{CF}^+ + \text{F} + \text{Ar}$	1.0×10^{-10}	estimated
$\text{CF} + \text{Ar}^+ \rightarrow \text{CF}^+ + \text{Ar}$	1.0×10^{-10}	estimated
$\text{H}_2\text{O} + \text{Ar}^+ \rightarrow \text{H}_2\text{O}^+ + \text{Ar}$	6.8×10^{-10}	[21]
$\text{H}_2\text{O} + \text{Ar}^+ \rightarrow \text{ArH}^+ + \text{OH}$	3.2×10^{-10}	[21]
$\text{CO} + \text{Ar}^+ \rightarrow \text{CO}^+ + \text{Ar}$	4.0×10^{-11}	[21]
$\text{CO}_2 + \text{Ar}^+ \rightarrow \text{CO}_2^+ + \text{Ar}$	4.4×10^{-10}	[21]
$\text{O}_2 + \text{Ar}^+ \rightarrow \text{O}_2^+ + \text{Ar}$	3.9×10^{-11}	[21]
$\text{O} + \text{Ar}^+ \rightarrow \text{O}^+ + \text{Ar}$	6.4×10^{-12}	[22, 23]
$\text{H}_2 + \text{Ar}^+ \rightarrow \text{ArH}^+ + \text{H}$	1.25×10^{-9}	[23]
$\text{H}_2\text{O} + \text{Ar}_2^+ \rightarrow \text{H}_2\text{O}^+ + 2\text{Ar}$	1.6×10^{-9}	[21]
$\text{CO} + \text{Ar}_2^+ \rightarrow \text{CO}^+ + 2\text{Ar}$	6.1×10^{-10}	[21]
$\text{CO}_2 + \text{Ar}_2^+ \rightarrow \text{CO}_2^+ + 2\text{Ar}$	7.7×10^{-10}	[21]
$\text{O}_2 + \text{Ar}_2^+ \rightarrow \text{O}_2^+ + 2\text{Ar}$	7.4×10^{-11}	[21]
$\text{H}_2 + \text{Ar}_2^+ \rightarrow \text{ArH}^+ + \text{H} + \text{Ar}$	3.6×10^{-10}	[24]
$\text{CF}_4 + \text{O}^+ \rightarrow \text{CF}_3^+ + \text{OF}$	1.4×10^{-9}	[8, 9]
$\text{H} + \text{O}^+ \rightarrow \text{H}^+ + \text{O}$	6.80×10^{-10}	[25]
$\text{H}_2\text{O} + \text{O}^+ \rightarrow \text{H}_2\text{O}^+ + \text{O}$	3.2×10^{-9}	[25]
$\text{O} + \text{H}^+ \rightarrow \text{O}^+ + \text{H}$	3.75×10^{-10}	[25]
$\text{H}_2\text{O} + \text{H}^+ \rightarrow \text{H}_2\text{O}^+ + \text{H}$	8.2×10^{-9}	[25]
$\text{O}_2 + \text{H}_2\text{O}^+ \rightarrow \text{O}_2^+ + \text{H}_2\text{O}$	2.5×10^{-10}	[26]
$\text{H}_2 + \text{H}_2\text{O}^+ \rightarrow \text{H}_3\text{O}^+ + \text{H}$	1.4×10^{-9}	[25]
$\text{H}_2\text{O} + \text{H}_2\text{O}^+ \rightarrow \text{H}_3\text{O}^+ + \text{OH}$	1.3×10^{-9}	[27]
$\text{H}_2\text{O} + \text{ArH}^+ \rightarrow \text{H}_3\text{O}^+ + \text{Ar}$	4.5×10^{-9}	[27]

at room temperature.

The ambient total pressure and temperature are 1 atm and 300 K, respectively. The concentration of CF_4 is 1000 ppm for all simulated cases. The concentration of added H_2O is 0 to 3%, near the saturated vapor pressure at $T = 300 \text{ K}$. The total gas density is $[\text{Ar}] + [\text{CF}_4] + [\text{H}_2\text{O}] = 2.45 \times 10^{19} \text{ cm}^{-3}$, where $[\text{X}]$ is the number density of X and $[\text{CF}_4] = 2.45 \times 10^{16} \text{ cm}^{-3}$.

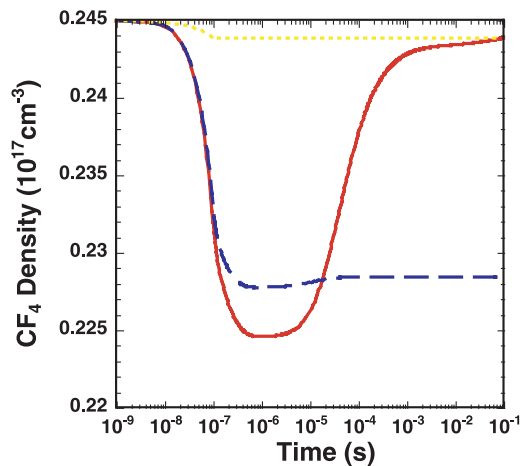
The input e-beam employs a square pulse, where the pulse width $\tau = 100 \text{ ns}$. It is assumed that all the input energy is used to excite the argon gas, as represented in by Eq. (1), because the concentrations of CF_4 and H_2O are less than about 1%.

4. Simulation Results

Figure 2 shows the time evolution of the CF_4 density for an input energy density of 20 mJ/cm^3 , when the concentration of H_2O is $1 \times 10^{-5}\%$, $2.5 \times 10^{-2}\%$, and 3%. Since the decay time of the activated species of argon is about 100 ns, the decomposition reaction of CF_4 is terminated within about 200 ns. Maximum decomposition is achieved when the concentration of H_2O is $1 \times 10^{-5}\%$. The number density of the decomposition is $2.0 \times 10^{15} \text{ cm}^{-3}$ and the concentration is about 80 ppm. The number density is in agreement with the estimated value presented in the previous section. However, most of the products of

Table 4 Electron attachment, dissociative recombination, and negative ion reaction processes. Electron attachment and dissociative recombination reaction depends on the electron temperature; for the processes discussed here, the electron temperature is around room temperature.

Reaction	Rate (cm ³ /s)	Ref.
CF ₃ + e ⁻ → CF ₂ + F ⁻	1×10 ⁻¹⁰	[28]
CF ₂ + e ⁻ → CF + F ⁻	1×10 ⁻¹⁰	[28]
CF + e ⁻ → C + F ⁻	1×10 ⁻¹⁰	[28]
F ₂ + e ⁻ → F + F ⁻	1.7×10 ⁻⁸	for 298 K [29]
CF ₃ ⁺ + e ⁻ → CF ₂ + F	2.08×10 ⁻⁷ ×(T/300 K) ^{-0.48}	[30, 31]
CF ₃ ⁺ + e ⁻ → CF + 2F	0.52×10 ⁻⁷ ×(T/300 K) ^{-0.48}	[30, 31]
CF ₂ ⁺ + e ⁻ → CF + F	2.63×10 ⁻⁷ ×(T/300 K) ^{-0.76}	[30, 31]
CF ₂ ⁺ + e ⁻ → C + 2F	1.07×10 ⁻⁷ ×(T/300 K) ^{-0.76}	[30, 31]
CF ⁺ + e ⁻ → C + F	0.52×10 ⁻⁷ ×(T/300 K) ^{-0.8}	[30, 32]
H ₂ O ⁺ + e ⁻ → OH + H	0.86×10 ⁻⁷ ×(T/300 K) ^{-0.74}	[30, 33]
H ₂ O ⁺ + e ⁻ → O + H ₂	0.39×10 ⁻⁷ ×(T/300 K) ^{-0.74}	[30, 33]
H ₂ O ⁺ + e ⁻ → O + 2H	3.05×10 ⁻⁷ ×(T/300 K) ^{-0.74}	[30, 33]
OH ⁺ + e ⁻ → O + H	0.375×10 ⁻⁷ ×(T/300 K) ^{-0.5}	[30, 34]
H ₃ O ⁺ + e ⁻ → H ₂ O + H	1.1×10 ⁻⁶ ×(T/300 K) ^{-0.5}	[27]
CO ₂ ⁺ + e ⁻ → CO ₂	0.26×10 ⁻⁷ ×(T/300 K) ^{-0.8}	[35]
CO ₂ ⁺ + e ⁻ → CO + O	5.65×10 ⁻⁷ ×(T/300 K) ^{-0.8}	[35]
CO ₂ ⁺ + e ⁻ → C + O ₂	0.59×10 ⁻⁷ ×(T/300 K) ^{-0.8}	[35]
CO ⁺ + e ⁻ → C + O	1.85×10 ⁻⁷	for 300 K [36]
O ₂ ⁺ + e ⁻ → 2O	1.95×10 ⁻⁷ ×(T/300 K) ^{-0.7}	[37]
ArH ⁺ + e ⁻ → Ar + H	7×10 ⁻¹⁰	for 5000 K [23]
Ar ₂ ⁺ + e ⁻ → Ar* + Ar	9.1×10 ⁻⁷ ×(T/300 K) ^{-0.61}	[17]
H + F ⁻ → HF + e ⁻	1.6×10 ⁻⁹	for 296 K [38]
CF ₃ ⁺ + F ⁻ → CF ₂ + F ₂	8.7 × 10 ⁻⁸	[28]
CF ₂ ⁺ + F ⁻ → CF + F ₂	9.1 × 10 ⁻⁸	[28]
CF ⁺ + F ⁻ → CF + F	9.8 × 10 ⁻⁸	[28]
O ₂ ⁺ + F ⁻ → F + O ₂	5 × 10 ⁻⁸	[39]
O ⁺ + F ⁻ → F + O ₂	5 × 10 ⁻⁸	[39]


 Fig. 2 Time evolution of CF₄ densities. The horizontal axis is logarithmic; the solid, dotted, and dashed lines represent H₂O concentrations of 1 × 10⁻³%, 2.5 × 10⁻²%, and 3%, respectively.

decomposition are reformed to CF₄ because of the small amount of additives. When the concentration of H₂O is 2.5 × 10⁻²%, the number density of the decomposition of CF₄ is 1.7 × 10¹⁵ cm⁻³. The decomposition efficiency decreases to 15% from the efficiency for an H₂O concentra-

tion of 1 × 10⁻⁵%. The carbon and fluorine atoms from the decomposition of CF₄ are efficiently converted to HF, CO₂, and other by-products using oxygen and hydrogen atoms from H₂O as the additives. In contrast, when the concentration of H₂O is 3%, most of the activated species of argon are consumed in the process of decomposing H₂O.

The variation in the density of CF₄ as a function of the H₂O concentration is shown in Fig. 3. The closed circles and triangles represent the minimum and final density of CF₄, respectively. Here, the final density refers to the density when the reformation of CF₄ is complete. For an input energy density of 20 mJ/cm³, the number density of the decomposition of CF₄ is maximum when the H₂O concentration is 2.5 × 10⁻²%. As the concentration of H₂O increases from 2.5 × 10⁻²%, the efficiency of the decomposition of CF₄ decreases, and most of the activated species of argon are consumed during decomposition of H₂O. As the concentration of H₂O decreases from 2.5 × 10⁻²%, the efficiency of the decomposition of CF₄ also decreases, and most decomposition products reform to CF₄.

The change in the concentration of CF₄ for input energy density is shown in Fig. 4. The concentration of H₂O is optimal for each input energy density. The temperature of the gas exceeds 500°C when the input energy density ex-

Table 5 Metastable and molecule reaction processes.

Reaction	Rate (cm ³ /s)	Ref.
CF ₄ + Ar* → CF ₂ + F ₂ + Ar	4.0×10 ⁻¹¹	[14]
CF ₃ + Ar* → CF ₂ + F + Ar	4.0×10 ⁻¹¹	estimated
CF ₂ + Ar* → CF + F + Ar	4.0×10 ⁻¹¹	estimated
F ₂ + Ar* → Ar + 2F	3.5×10 ⁻¹⁰	[40]
F ₂ + Ar* → ArF* + F	4.0×10 ⁻¹⁰	[40]
H ₂ O + Ar* → O + 2H + Ar	1.84×10 ⁻¹⁰	[41–43]
H ₂ O + Ar* → OH + H + Ar	2.16×10 ⁻¹⁰	[41–43]
O ₂ + Ar* → 2O + Ar	2.2×10 ⁻¹⁰	[42]
CO + Ar* → C + O + Ar	2.7×10 ⁻¹¹	[42]
CO ₂ + Ar* → CO + O + Ar	5.6×10 ⁻¹⁰	[42]
F ₂ + Ar ₂ * → Ar ₂ F* + F	2.5×10 ⁻¹⁰	[44, 45]
F ₂ + Ar ₂ * → ArF* + F + Ar	3.0×10 ⁻¹⁰	[44]
F + Ar ₂ * → ArF* + Ar	3.0×10 ⁻¹⁰	[44, 45]
H ₂ O + Ar ₂ * → OH + H + 2Ar	1.4×10 ⁻⁹	[46]
O ₂ + Ar ₂ * → 2O + 2Ar	2.6×10 ⁻¹⁰	[18]
CO + Ar ₂ * → CO + 2Ar	1.6×10 ⁻¹⁰	[18]
CO ₂ + Ar ₂ * → CO + O + 2Ar	6.8×10 ⁻¹⁰	[18]
Ar* + Ar* → Ar ⁺ + Ar + e ⁻	5.0×10 ⁻¹⁰	[47]
Ar ₂ * + Ar ₂ * → Ar ₂ ⁺ + 2Ar + e ⁻	5.0×10 ⁻¹⁰	[47]
Ar* + Ar ₂ * → Ar ⁺ + 2Ar + e ⁻	5.0×10 ⁻¹⁰	[47]
ArF* + (Ar) → Ar + F + (Ar)	9.0×10 ⁻¹²	[48, 49]
Ar ₂ F* + (Ar) → 2Ar + F + (Ar)	2.2×10 ⁻¹⁴	[50]
Ar ₂ * + (e ⁻) → 2Ar + (e ⁻)	1.0×10 ⁻⁹	[51]
ArF* + (e ⁻) → Ar + F + (e ⁻)	1.6×10 ⁻⁷	[52]
Ar ₂ F* + (e ⁻) → 2Ar + F + (e ⁻)	1.0×10 ⁻⁷	[44]
Ar ₂ * → 2Ar + hv	6.0×10 ⁶ s ⁻¹	[19]
ArF* → Ar + F + hv	2.50×10 ⁸ s ⁻¹	[45]
Ar ₂ F* → 2Ar + F + hv	4.3×10 ⁶ s ⁻¹	[50]

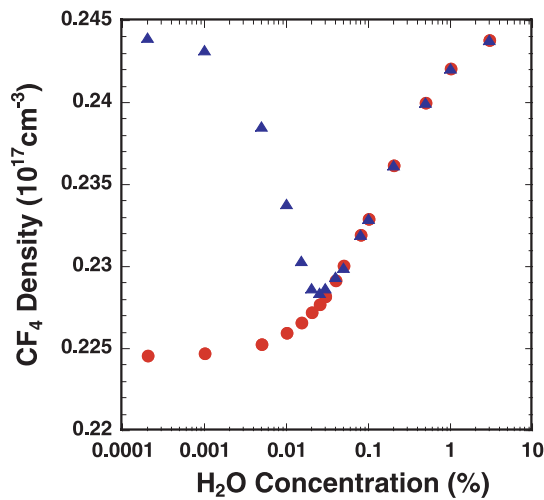


Fig. 3 Variations in the density of CF₄ as a function of the concentration of H₂O. Closed circles and triangles represent the minimum and final density of CF₄, respectively. The time of the final density is 100 ms.

ceeds 200 mJ/cm³ (no cooling is applied). It was assumed for simplicity that the temperature of the gas is unchanged; that is, the same reaction rates are used. A final CF₄ decomposition of 99% is obtained for an input energy density of 1 J/cm³. This input energy density of 1 J/cm³ cor-

Table 6 Radical and molecule reaction processes; gas temperature is 300 K.

Reaction	Rate (cm ³ /s)	Ref.
CF ₃ + O → COF ₂ + F	3.11×10 ⁻¹¹	[53]
CF ₂ + O → COF + F	1.4×10 ⁻¹¹	[54, 55]
CF ₂ + O → CO + 2F	4×10 ⁻¹²	[54, 55]
CF + O → CO + F	3.9×10 ⁻¹¹	[56]
COF + O → CO ₂ + F	9.3×10 ⁻¹¹	[54, 55]
CF ₃ + H → CF ₂ + HF	9.1×10 ⁻¹¹	[57]
CF ₂ + H → CF + HF	3.9×10 ⁻¹¹	[57]
CF + H → C + HF	1.9×10 ⁻¹¹	[57]
CF ₃ + F ₂ → CF ₄ + F	7.0×10 ⁻¹⁴	[58]
CF + F ₂ → CF ₂ + F	3.9×10 ⁻¹²	[59]
C + F ₂ → CF + F	2.3×10 ⁻¹²	extrapolated
H + F ₂ → HF + F	1.5×10 ⁻¹²	[60]
F + H ₂ → HF + H	2.5×10 ⁻¹¹	[61]
F + H ₂ O → OH + HF	1.4×10 ⁻¹¹	[61]
OF + O → O ₂ + F	2.7×10 ⁻¹¹	[62, 63]
OF + H → HF + O	8.2×10 ⁻¹²	[64]
OF + OF → O ₂ + F ₂	4.6×10 ⁻¹⁵	[65]
COF + CF ₂ → CF ₃ + CO	3×10 ⁻¹³	[55]
COF + CF ₂ → COF ₂ + CF	3×10 ⁻¹³	[55]
COF + CF ₃ → CF ₄ + CO	1×10 ⁻¹¹	[55]
COF + CF ₃ → COF ₂ + CF ₂	1×10 ⁻¹¹	[55]
COF + COF → COF ₂ + CO	1×10 ⁻¹¹	[55]
OH + OH → H ₂ O + O	1.47×10 ⁻¹²	[66]
OH + O → O ₂ + H	3.5×10 ⁻¹¹	[66]
C + O ₂ → CO + O	1.6×10 ⁻¹¹	[67]
H ₂ O ₂ + H → H ₂ O + OH	4.2×10 ⁻¹⁴	[68]
H ₂ O ₂ + H → H ₂ + HO ₂	5.15×10 ⁻¹⁵	[68]
H ₂ O ₂ + O → OH + HO ₂	1.78×10 ⁻¹⁵	[66]
H ₂ O ₂ + OH → H ₂ O + HO ₂	1.7×10 ⁻¹²	[66]
HO ₂ + H → H ₂ + O ₂	5.6×10 ⁻¹²	[66]
HO ₂ + H → 2OH	7.2×10 ⁻¹¹	[66]
HO ₂ + H → H ₂ O + O	2.4×10 ⁻¹²	[66]
HO ₂ + O → OH + O ₂	5.7×10 ⁻¹¹	[66]
HO ₂ + OH → H ₂ O + O ₂	1.1×10 ⁻¹⁰	[66]
HO ₂ + HO ₂ → H ₂ O ₂ + O ₂	1.63×10 ⁻¹²	[66]

responds to an energy efficiency for CF₄ decomposition of 13 g/kWh.

5. Concluding Remarks

In this paper, we developed a computational method using a kinetic model of CF₄ in wet argon gas under e-beam irradiation. It was found that the activated species Ar⁺ and Ar* decompose CF₄, and the concentration of H₂O can be optimized for the decomposition of CF₄. The energy efficiency for CF₄ decomposition was 13 g/kWh for 99% of CF₄ concentration of 1000 ppm in an atmospheric-pressure argon gas.

The reaction of the activated species of argon with primary products such as CF_n (n = 1, 2, 3.) are included in the current model. However, the reaction rates are estimated since the actual reaction rates are unknown. Secondary products, such as COF₂, are not included in the model because the activated species of argon are quenched

Table 7 Three-body reaction rate processes. The pressure and temperature of argon buffer gas were 760 torr and 300 K. The number density of Ar was $2.45 \times 10^{19} \text{ cm}^{-3}$. The unit of reaction rate is cm^6/s when the reaction rates depend quasi-linearly on the buffer gas density. The unit of reaction rate is cm^3/s when the reaction rates depend nonlinearly on the buffer gas density.

Reaction	Rate	Ref.
$\text{Ar}^+ + \text{Ar} (+\text{Ar}) \rightarrow \text{Ar}_2^+ (+\text{Ar})$	0.7×10^{-31}	[16]
$\text{Ar}^* + \text{Ar} (+\text{Ar}) \rightarrow \text{Ar}_2^* (+\text{Ar})$	1.0×10^{-32}	[18]
$\text{ArF}^* + \text{Ar} (+\text{Ar}) \rightarrow \text{Ar}_2\text{F}^* (+\text{Ar})$	4.0×10^{-31}	[48, 49]
$\text{Ar}^+ + \text{F}^- (+\text{Ar}) \rightarrow \text{ArF}^* (+\text{Ar})$	3.3×10^{-6}	[69]
$\text{Ar}_2^+ + \text{F}^- (+\text{Ar}) \rightarrow \text{ArF}^* + \text{Ar} (+\text{Ar})$	2.9×10^{-6}	[70]
$\text{CF}_3 + \text{F} (+\text{M}) \rightarrow \text{CF}_4 (+\text{M})$	1.9×10^{-11}	[55]
$\text{CF}_2 + \text{F} (+\text{M}) \rightarrow \text{CF}_3 (+\text{M})$	1.2×10^{-11}	[55]
$\text{CF} + \text{F} (+\text{M}) \rightarrow \text{CF}_2 (+\text{M})$	3.2×10^{-12}	[55]
$\text{COF} + \text{F} (+\text{M}) \rightarrow \text{COF}_2 (+\text{M})$	1.3×10^{-11}	[55]
$\text{CO} + \text{F} (+\text{M}) \rightarrow \text{COF} (+\text{M})$	1.8×10^{-12}	[55]
$\text{F} + \text{F} (+\text{M}) \rightarrow \text{F}_2 (+\text{M})$	6.0×10^{-34}	[71]
$\text{OH} + \text{OH} (+\text{M}) \rightarrow \text{H}_2\text{O}_2 (+\text{M})$	2×10^{-31}	analogous to N_2 [72]
$\text{OH} + \text{H} (+\text{M}) \rightarrow \text{H}_2\text{O} (+\text{M})$	2.6×10^{-31}	[72]
$\text{H} + \text{O}_2 (+\text{M}) \rightarrow \text{HO}_2 (+\text{M})$	2.0×10^{-32}	[72]
$\text{H} + \text{H} (+\text{M}) \rightarrow \text{H}_2 (+\text{M})$	6.0×10^{-33}	[72]
$\text{O} + \text{O} (+\text{M}) \rightarrow \text{O}_2 (+\text{M})$	1.1×10^{-33}	[73]
$\text{CO} + \text{O} (+\text{M}) \rightarrow \text{CO}_2 (+\text{M})$	9.8×10^{-36}	[74]

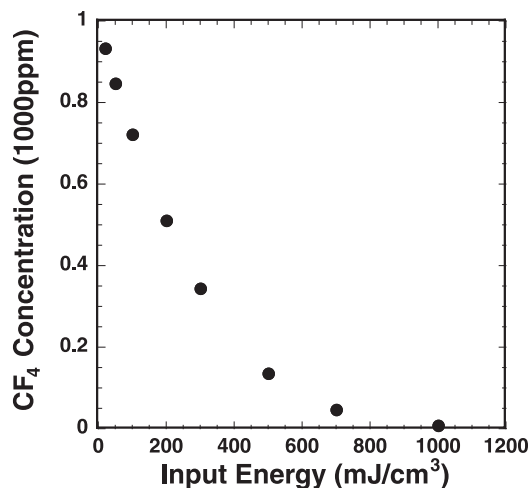


Fig. 4 Concentration of CF_4 at 100 ms as a function of input energy density.

before the secondary products are produced. The assumption applies to an e-beam pulse width less than $1 \mu\text{s}$; thus the model can be applied when the e-beam pulse width is less than $1 \mu\text{s}$.

The rate of formation of Ar_2^+ from Ar^+ is crucial in the efficient reaction of the decomposition of CF_4 . The ion-molecule reaction rate coefficients of three-body ion atom association in argon gas were obtained, and the range was from 0.6 to $5 \times 10^{-31} \text{ cm}^6/\text{s}$ [75]. We use the value $0.7 \times 10^{-31} \text{ cm}^6/\text{s}$ [16] in the simulation. If, however, we use $2.0 \times 10^{-31} \text{ cm}^6/\text{s}$ [76], the maximum number density of decomposed CF_4 for an input energy of $20 \text{ mJ}/\text{cm}^3$ decreases to $1.3 \times 10^{15} \text{ cm}^{-3}$ from $2.0 \times 10^{15} \text{ cm}^{-3}$.

- [1] M.B. Chang and J.-S. Chang, *Ind. Eng. Chem. Res.* **45**, 4101 (2006).
- [2] B.M. Penetrante, M.C. Hsiao, J.N. Bardsley, B.T. Merritt, G.E. Vogtlin, P.H. Wallman, A. Kuthi, C.P. Burkhardt and J.B. Bayless, *Phys. Lett. A* **209**, 69 (1995).
- [3] R. Hermann, *Radiat. Phys. Chem.* **34**, 369 (1989).
- [4] R. Hermann, *Radiat. Phys. Chem.* **36**, 227 (1990).
- [5] R.A. Bonham, *Jpn. J. Appl. Phys.* **33**, 4157 (1994).
- [6] D.C. Lorents, *Physica C* **82**, 19 (1976).
- [7] E.R. Fisher, M.E. Weber and P.B. Armentrout, *J. Chem. Phys.* **92**, 2296 (1990).
- [8] X.P. Xu, S. Rauf and M.J. Kushner, *J. Vac. Sci. Technol. A: Vac. Surf. Films* **18**, 213 (2000).
- [9] E.R. Fisher and P.B. Armentrout, *J. Phys. Chem.* **95**, 6118 (1991).
- [10] M. Chau and M.T. Bowers, *Int. J. Mass. Spectrom. Ion Phys.* **24**, 191 (1977).
- [11] R.A. Morris, A.A. Viggiano, S.T. Arnold and J.F. Paulson, *Int. J. Mass Spectrom. Ion Process* **149/150**, 287 (1995).
- [12] R.A. Morris, A.A. Viggiano, J.M. Van Doren and J.F. Paulson, *J. Phys. Chem.* **96**, 3051 (1992).
- [13] J.E. Velazco, J.H. Kolts and D.W. Setser, *J. Chem. Phys.* **69**, 4357 (1978).
- [14] L.G. Piper, J.E. Velazco and D.W. Setser, *J. Chem. Phys.* **59**, 3323 (1973).
- [15] V.I. Sorokin, N.P. Gritsan and A.I. Chichinin, *J. Chem. Phys.* **108**, 8995 (1998).
- [16] Jen-Shih Chang, Y. Ichikawa, R.M. Hobson, S. Matsumura and S. Teii, *J. Appl. Phys.* **72**, 2632 (1992).
- [17] Yueh-Jaw Shiu and M.A. Biondi, *Phys. Rev. A* **17**, 868 (1978).
- [18] T. Oka, M. Kogoma, M. Imamura, S. Arai and T. Watanabe, *J. Chem. Phys.* **70**, 3384 (1979).
- [19] J.W. Keto, R.E. Gleason and G.K. Walters, *Phys. Rev. Lett.* **33**, 1365 (1974).
- [20] I. Okuda, *Rev. Laser Eng.* **32**, 271 (2004) [in Japanese].
- [21] R.J. Shul, B.L. Upschulte, R. Passarella, R.G. Keesee and

- A.W. Castleman, *J. Phys. Chem.* **91**, 2556 (1987).
- [22] A.V. Vasenkov, Xi Li, G.S. Oehrlein and M.J. Kushner, *J. Vac. Sci. Technol. A: Vac. Surf. Films* **22**, 511 (2004).
- [23] P. Gaucherel and B. Rowe, *Int. J. Mass. Spectrom. Ion Phys.* **25**, 227 (1977).
- [24] R.J. Shul, R. Passarella, B.L. Upschulte, R.G. Keesee and A.W. Castleman Jr., *J. Chem. Phys.* **86**, 4446 (1987).
- [25] V.G. Anicich and W.T. Huntress Jr, *Astrophys. J. Suppl. Ser.* **62**, 553 (1986).
- [26] G.B.I. Scott, D.A. Fairley, D.B. Milligan, C.G. Freeman and J. Murray, *J. Phys. Chem. A* **103**, 7470 (1999).
- [27] W. Lindinger, *Phys. Rev. A* **7**, 328 (1973).
- [28] G.I. Font, W.L. Morgan and G. Mennenga, *J. Appl. Phys.* **9**, 3530 (2002).
- [29] D.L. McCorkle, L.G. Christophorou, A.A. Christodoulides and L. Pichiarella, *J. Chem. Phys.* **85**, 1966 (1986).
- [30] A.I. Florescu-Mitchell and J.B.A. Mitchell, *Phys. Rep.* **430**, 277 (2006).
- [31] A. Ehlerding, A.A. Viggiano, F. Hellberg, R.D. Thomas, V. Zhaunerchyk, W.D. Geppert, H. Montaigne, M. Kaminska, F. Österdahl, M. afUgglas, M. Larsson, O. Novotny, J.B.A. Mitchell, J.L. LeGarrec, A.I. Florescu-Mitchell, C. Rebrion-Rowe, A. Svendsen, M.A. ElGhazaly and L.H. Andersen, *J. Phys. B: Atomic Mol. Opt. Phys.* **39**, 805 (2006).
- [32] O. Novotny, J.B.A. Mitchell, J.L. LeGarrec, A.I. Florescu-Mitchell, C. Rebrion-Rowe, A. Svendsen, M.A. ElGhazaly, L.H. Andersen, A. Ehlerding, A.A. Viggiano, F. Hellberg, R.D. Thomas, V. Zhaunerchyk, W.D. Geppert, H. Montaigne, M. Kaminska, F. Österdahl and M. Larsson, *J. Phys. B: Atomic Mol. Opt. Phys.* **38**, 1471 (2005).
- [33] S. Rosén, A. Derkach, J. Semaniak, A. Neau, A. Al-Khalili, A. LePadellec, L. Viktor, R. Thomas, H. Danared, M. afUgglas and M. Larsson, *Faraday Discuss.* **115**, 295 (2000).
- [34] P.M. Mul, J.W. McGowan, P. DeFrance and J.B.A. Mitchell, *J. Phys. B: Atomic Mol. Opt. Phys.* **16**, 3099 (1983).
- [35] A.A. Viggiano, A. Ehlerding, F. Hellberg, R.D. Thomas, V. Zhaunerchyk, W.D. Geppert, H. Montaigne, M. Larsson, M. Kaminska and F. Osterdahl, *J. Chem. Phys.* **122**, 226101 (2005).
- [36] S. Laubé, L. Lehfaoui, B.R. Rowe and J.B.A. Mitchell, *J. Phys. B: Atomic Mol. Opt. Phys.* **31**, 4181 (1998).
- [37] F.J. Mehr and A. Manfred, *Phys. Rev.* **181**, 264 (1969).
- [38] F.C. Fehsenfeld, C.J. Howard and E.E. Ferguson, *J. Chem. Phys.* **58**, 5841 (1973).
- [39] T.J. Sommerer and M.J. Kushner, *J. Appl. Phys.* **71**, 1654 (1992).
- [40] J.H. Kolts and D.W. Setser, *J. Phys. Chem.* **82**, 1766 (1978).
- [41] M. Bourene and J. Le Calvé, *J. Chem. Phys.* **58**, 1452 (1973).
- [42] J. Balamuta and M.F. Golde, *J. Chem. Phys.* **76**, 2430 (1982).
- [43] J. Balamuta, M.F. Golde and Yueh-Se Ho, *J. Chem. Phys.* **79**, 2822 (1983).
- [44] F. Kannari, M. Obara and T. Fujioka, *J. Appl. Phys.* **57**, 4309 (1985).
- [45] T.H. Johnson and A.M. Hunter II, *J. Appl. Phys.* **51**, 2406 (1980).
- [46] J.B. Leblond, F. Collier, F. Hobeck and P. Cottin, *J. Chem. Phys.* **74**, 6242 (1981).
- [47] S.K. Lam, C.E. Zheng, D. Lo, A. Dem'yanov and A.P. Napartovich, *J. Phys. D: Appl. Phys.* **33**, 242 (2000).
- [48] M. Rokni, J.H. Jacob, J.A. Mangano and R. Brochu, *Appl. Phys. Lett.* **31**, 79 (1977).
- [49] M. Rokni, J.H. Jacob and J.A. Mangano, *Phys. Rev.* **A16**, 2216 (1977).
- [50] N. Boewering, R. Sauerbrey and H. Langho, *J. Chem. Phys.* **76**, 3524 (1982).
- [51] J.W. Wilson and A. Shapiro, *J. Appl. Phys.* **51**, 2387 (1980).
- [52] D.W. Trainor and J.H. Jacob, *Appl. Phys. Lett.* **37**, 675 (1980).
- [53] C.P. Tsai, S.M. Belanger, J.T. Kim, J.R. Lord and D.L. McFadden, *J. Phys. Chem.* **93**, 1916 (1989).
- [54] K.R. Ryan and I.C. Plumb, *Plasma Chem. Plasma Process.* **4**, 271 (1984).
- [55] I.C. Plumb and K.R. Ryan, *Plasma Chem. Plasma Process.* **6**, 205 (1986).
- [56] J.V. Hoeymissen, I.D. Boelpaep, W. Uten and J. Peeters, *J. Phys. Chem.* **98**, 3725 (1994).
- [57] C.P. Tsai and D.L. McFadden, *J. Phys. Chem.* **93**, 2471 (1986).
- [58] I.C. Plumb and K.R. Ryan, *Plasma Chem. Plasma Process.* **6**, 11 (1986).
- [59] J. Peeters, J. Van Hoeymissen, S. Vanhaelemeersch and D. Vermeylen, *J. Phys. Chem.* **96**, 1257 (1992).
- [60] N. Cohen and K.R. Westberg, *J. Phys. Chem. Ref. Data* **12**, 531 (1983).
- [61] R. Atkinson, D.L. Baulch, R.A. Cox, J.N. Crowley, R.F. Hampson, R.G. Hynes, M.E. Jenkin, M.J. Rossi and J. Troe, *ACP* **7**, 981 (2007).
- [62] R. Atkinson, D.L. Baulch, R.A. Cox, R.F. Hampson Jr., J.A. Kerr, M.J. Rossi and J. Troe, *J. Phys. Chem. Ref. Data* **26**, 521 (1997).
- [63] JPL, S.P. Sander, R.R. Friedl, D.M. Golden, M.J. Kurylo, G.K. Moortgat, H. Keller-Rudek, P.H. Wine, A.R. Ravishankara, C.E. Kolb, M.J. Molina, B.J. Finlayson-Pitts, R.E. Huie and V.L. Orkin, *JPL Publication* **06**, 1 (2006).
- [64] Yu.R. Bedzhanyan, E.M. Markin and Yu.M. Gershenzon, *Kinet. Catal.* **33**, 802 (1993).
- [65] A.J. Colussi and M.A. Grela, *Chem. Phys. Lett.* **229**, 134 (1994).
- [66] R. Atkinson, D.L. Baulch, R.A. Cox, J.N. Crowley, R.F. Hampson, R.G. Hynes, M.E. Jenkin, M.J. Rossi and J. Troe, *ACP* **4**, 1461 (2004).
- [67] G. Dorthe, P. Caubet, T. Vias, B. Barrere and J. Marchais, *J. Phys. Chem.* **95**, 5109 (1991).
- [68] D.L. Baulch, C.J. Cobos, R.A. Cox, C. Esser, P. Frank, Th. Just, J.A. Kerr, M.J. Pilling, J. Troe, R.W. Walker and J. Warnatz, *J. Phys. Chem. Ref. Data* **21**, 411 (1992).
- [69] M.R. Flannery and T.P. Yang, *Appl. Phys. Lett.* **32**, 327 (1978).
- [70] M.R. Flannery and T.P. Yang, *Appl. Phys. Lett.* **32**, 356 (1978).
- [71] C.J. Ultee, *Chem. Phys. Lett.* **46**, 366 (1977).
- [72] D.L. Baulch, C.T. Bowman, C.J. Cobos, R.A. Cox, Th. Just, J.A. Kerr, M.J. Pilling, D. Stocker, J. Troe, W. Tsang, R.W. Walker and J. Warnatz, *J. Phys. Chem. Ref. Data* **34**, 757 (2005).
- [73] W. Tsang and R.F. Hampson, *J. Phys. Chem. Ref. Data* **15**, 1087 (1986).
- [74] E.C.Y. Inn, *J. Chem. Phys.* **59**, 5431 (1973).
- [75] W.F. Liu and D.C. Conway, *J. Chem. Phys.* **60**, 784 (1974).
- [76] K. Hiraoka and T. Mori, *J. Chem. Phys.* **90**, 7143 (1989).